Inorganic Chemistry

Article

pubs.acs.org/IC

Varying Substituents and Solvents To Maximize the Luminescence from [Ru(trpy)(bpy)CN]$^+$ Derivatives

Matthew A. Bork, Hunter B. Vibbert, David J. Stewart, Phillip E. Fanwick, and David R. McMillin*

Department of Chemistry, Purdue University, 560 Oval Drive, West Lafayette, Indiana 47907-2084, United States

Supporting Information

ABSTRACT: Ruthenium(II) in combination with monodentate, bidentate, and tridentate ligands has proven to be a useful design for a variety of applications, but the majority of systems are virtually nonluminescent in solution. The goal of this work has been to design luminescent forms with practicable emission quantum yields, and the focus has been on [Ru(X-T)(dmeb)CN]$^+$ systems, where X-T denotes 2,2′:6′,2″-terpyridine bearing substituent X at the 4′-position and dmeb denotes [2,2′-bipyridine]-4,4′-dicarboxylic acid, dimethyl ester. Results show that varying the π-electron-donating ability of the 4′-X substituent is an effective way to tune the energy and lifetime of the charge-transfer (CT) emission. The lifetime achieved in a room-temperature, fluid solution is as high as 175 ns, depending on the 4′-substituent and the solvent employed because the excited state is very polar. That represents a 20-fold improvement in lifetime relative to that of the prototype, [Ru(trpy)(bpy)CN]$^+$, one of the earliest examples found to be luminescent in a fluid solution. A simple theoretical model proves to be capable of rationalizing all the experimental lifetimes. It suggests that, with the dmeb ligand available to accept the electron, enhancing the donor ability of the 4′-X substituent lowers the energy of the ^{3}CT state and reduces the likelihood of thermally activated decay via a higher-energy d−d state. However, direct nonradiative decay to the ground state begins to reduce the excited-state lifetime whenever the emission maximum shifts beyond 750 nm. Within those limits, there is inevitably a maximal attainable lifetime, regardless of the method of tuning.

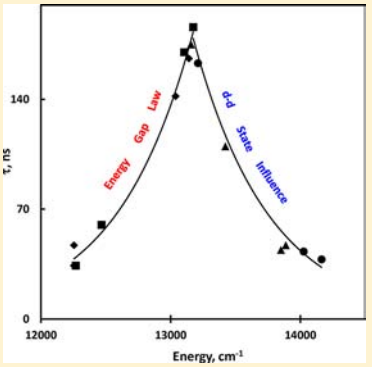

INTRODUCTION

The exploration of the photochemical and photophysical properties of polypyridine complexes of ruthenium(II) is a quest with a long history.[1−3] Early on, the [Ru(trpy)$_2$]$^{2+}$ system, where trpy denotes 2,2′:6′,2″-terpyridine, came to the fore as an unusual example of a ruthenium polypyridine that has a strong metal-to-ligand charge-transfer (MLCT) absorption spectrum in the visible but a very short excited-state lifetime ($\tau \approx 250$ ps) in a fluid solution.[4] Experiments have shown that facile, thermally assisted deactivation via a low-lying d−d excited state accounts for the short charge-transfer (CT) excited-state lifetime as well as the absence of a luminescence signal.[5,6] The low-lying d-d excited state occurs because the trpy framework compromises metal−ligand σ bonding by imposing suboptimal N−Ru−N″ bite angles, i.e., bond angles involving the outer nitrogen atoms of trpy, that are only ∼160°.[7−9] Subsequent work involving the replacement of nitrogen donor centers with carbon or expanding the trpy framework has produced analogues with long-lived excited states, but the results have varied widely.[10−13] Taking a subtler approach and keeping the donor atoms intact, Maestri et al. have shown that decorating bis-terpyridine complexes of ruthenium(II) with appropriate combinations of peripheral, electronically active substituents also promotes the observation of emission signals and excited-state lifetimes as long as 50 ns in a fluid solution.[14] Because of the presence of only one trpy ligand, the strain effect is somewhat weaker in thermally stable, quaternary complexes of the type [Ru(trpy)(bpy)L]$^{2+}$, where bpy denotes 2,2′-bipyridine and L is a neutral ligand such as acetonitrile. Nonetheless, the d−d excited state remains accessible, and the population of the d−d state can give rise to the photoinduced loss of L by a dissociative process with a modest quantum yield.[15] Reattachment of ligand L is possible, and Sauvage and co-workers have utilized [Ru(trpy)(bpy)L]$^{2+}$ systems in attempts to develop photoresponsive molecular devices.[16] Goldbach et al. have also used a similar platform for the development of ruthenium-based photoactivatable drugs.[17] Incorporating dimethyl sulfoxide as the monodentate ligand produces a photochromic system based on linkage isomerization of the sulfoxide ligand.[18]

Other work has also shown that related systems, including [Ru(trpy)(bpy)(CN)]$^+$ and [Ru(trpy)(bpy)(pyridine)]$^{2+}$, exhibit short-lived CT emission in solution.[19,20] More recently, Stewart et al. have reported an analogue that functions as a DNA light switch.[21] Along with the work of Maestri et al.,[14] those reports provide the motivation for the attempted optimization of photoluminescence properties described herein. The systems under investigation have the composition [Ru(X-T)(dmeb)(CN)]$^+$, where X-T denotes a 4-substituted 2,2′:6′,2″-terpyridine and dmeb denotes [2,2′-bipyridine]-4,4′-dicarboxylic acid, dimethyl ester (Scheme 1). Our findings

Received: July 1, 2013
Published: October 15, 2013

   dx.doi.org/10.1021/ic4016367 | Inorg. Chem. 2013, 52, 12553−12560

Scheme 1

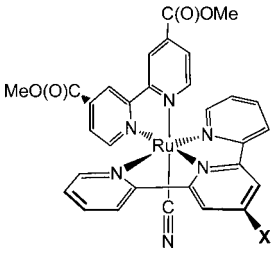

X	X-T
$-C_6H_5$	Ph-T
$-NMe_2$	dma-T
	pyrr-T

show that the emission lifetime varies strongly with the 4′-substituent on trpy as well as the solvent and that the lifetime tops out at ∼175 ns. Deactivation via thermally accessible d−d states and/or the energy gap law limits the lifetime, depending on the energy of the emitting CT state.

EXPERIMENTAL SECTION

Materials. Reagents ruthenium(III) trichloride hydrate, 2,2′:6′,2″-terpyridine, and trimethylamine *N*-oxide dihydrate (TMANO) were supplied by Aldrich Chemical Co. The supplier of 4′-chloro-2,2′:6′,2″-terpyridine was Acros, while 4,4′-dimethyl-2,2′-bipyridine was from G. Frederick Smith Chemical Co. Sigma-Aldrich supplied AgCN, pyrrolidine, tetrabutylammonium hexafluorophosphate ($TBAPF_6$), ferrocene, formic acid, and KPF_6. Most solvents, including methanol, acetone, dimethyl sulfoxide (DMSO), dichloromethane (DCM), and chloroform, were commercial products from Mallinckrodt, as were H_2SO_4 and $K_2Cr_2O_7$. Macron supplied the dimethylformamide (DMF). Exciton supplied the Coumarin 480 laser dye.

Instrumentation. The instrument used to measure UV−visible absorption spectra was a Varian Cary 100 spectrometer. The fluorescence spectrophotometer was a Varian Cary Eclipse model equipped with an R3896 phototube. The VSL-337-NDS nitrogen dye laser and DLM-220 dye attachment were from Laser Science. The detection system for emission decay included a Hamamatsu R928 phototube, a Pacific Instruments model 277 high-voltage supply, and a Tectronix TDS 520 digitizing oscilloscope. For short-lived emission, the instrument of choice was an Optical Building Blocks EasyLife V apparatus in conjunction with a 435 nm LED. The mass spectrometer was a Waters Micromass ZQ ESI mass spectrometer with a single quadrupole. The cone voltage setting was typically 40 V. The NMR spectrometer was a Varian Inova300 spectrometer. A CHI620A voltammetric analyzer produced cyclic voltammograms, in conjunction with a Pt-wire auxiliary electrode, a Ag/AgCl reference electrode, and a platinum working electrode. The diffractometer was a Rigaku Rapid II instrument equipped with confocal optics. Galbraith Laboratories, Inc. (Nashville, TN), or Midwest Microlab, LLC (Indianapolis, IN), performed all elemental analyses.

Methods. The method of Parker and Rees provided estimates of emission quantum yields, with $[Ru(bpy)_3]^{2+}$ dissolved in acetonitrile as a standard (Φ = 0.062).[22,23] The manufacturer supplied emission correction factors for the spectrophotometer. Purging the solution with nitrogen gas sufficed for deoxygenation in a cuvette sealed with a septum. The electrolyte for cyclic voltammetry was 0.1 M $TBAPF_6$ in DMF. The sample concentrations were 1.0 mM, and the external reference was ferrocenium/ferrocene, which appeared at 0.56 V in DMF in the same electrolyte. Multiplying the emission intensity at wavelength λ by λ^2 allowed for conversion from nanometers to an inverse centimeter scale.[24] In optimizing the fit of the measured rate constants for decay, k_d, to a theoretical model, we assumed that the percentage error in the k_d values is constant. Thus, the computation of χ^2 depends on summing over the squares of weighted residuals, $(k_d - k)/k_d$, where k is a calculated value that is derived from the model.

The methods for synthesizing $[Ru(CO)_2Cl_2]_n$,[25] dmeb ([2,2′-bipyridine]-4,4′-dicarboxylicacid, 4,4′-dimethyl ester),[26,27] dma-T (4′-dimethylamino-2,2′:6′,2″-terpyridine),[28,29] and pyrr-T [4′-(pyrrolidin-1-yl)-2,2′:6′,2″-terpyridine][30] were from the literature. The 4′-phenyl-2,2′:6′,2″-terpyridine (Ph-T) ligand was available from a previous study.[31] The following synthetic procedures are representative of those used for all complexes in this study.

cis-(CO)-[Ru(pyrr-T)(CO)$_2$Cl]PF$_6$. Chelation of the tridentate ligand occured upon mixing pyrr-T (0.080 g, 0.264 mmol) and $[Ru(CO)_2Cl_2]_n$ (0.054 g, 0.24 mmol) and refluxing in a 3:1 MeOH/$CHCl_3$ solution for 18 h in the dark. After addition of 20 mL of water and evaporation of the organic solvents, the desired complex precipitated upon addition of excess KPF_6(aq). After dissolution in acetone, the addition of diethyl ether induced precipitation of the material suitable for preparative use.

[Ru(pyrr-T)(dmeb)Cl]PF$_6$. Synthesis of the complex begins with combining dmeb (0.065 g, 0.277 mmol) and $[Ru(pyrr\text{-}T)(CO)_2Cl_2]$-$PF_6$ (0.125 g, 0.227 mmol) in 150 mL of MeOH. Addition of TMANO (0.310 g, 2.2 mmol) initiates the replacement of carbon monoxide with dmeb, which takes place during a 15 h reflux. The desired complex precipitates with the addition of excess KPF_6(aq) after the addition of 20 mL of water and evaporation of the methanol.

[Ru(pyrr-T)(dmeb)CN]PF$_6$. Preparation begins with combining $[Ru(pyrr\text{-}T)(dmeb)Cl]PF_6$ (0.075 g, 0.08 mmol) with a 10-fold excess AgCN (100 mg, 0.9 mmol) in 200 mL of acetonitrile. Refluxing for 24 h induces the exchange of chloride with cyanide. Filtration removes insoluble silver salts. The addition of 20 mL of water followed by evaporation of acetonitrile and addition of excess KPF_6(aq) yields the crude product. Column chromatography on silica proves to be an effective technique for purification. Eluting with pure methanol removes a yellow band, and then a purple band elutes with 0.01 M NaCl in methanol. A presumably dicationic species remains on the column as a red band. After anion metathesis, recrystallization by slow evaporation from a 2:1 acetone/*n*-propanol mixture yields an analytically pure product.

[Ru(trpy)(dmeb)CN]PF$_6$. ^{1}H NMR [300 MHz, $(CD_3)_2SO$]: δ 10.13 (d, 1H), 9.33 (s, 1H), 9.14 (s, 1H), 8.86 (d, 2H), 8.72 (d, 2H), 8.42 (dd, 1H), 8.36 (t, 1H), 8.05 (dd, 2H), 7.67 (d, 2H), 7.61 (d, 1H), 7.54 (d, 1H), 7.37 (dd, 2H), 4.08 (s, 3H), 3.86 (s, 3H). ESI-MS (632.61 calcd for $C_{30}H_{23}N_6O_4Ru^+$) m/z (%): 632.79 (100) [M]. Anal. Found: C, 45.82; H, 3.26; N, 10.14. Calcd for $C_{30}H_{23}F_6N_6O_4PRu\cdot H_2O\cdot 0.5C_3H_8O$: C, 45.82; H, 3.54; N, 10.18. Molar extinction coefficient: ε (497 nm) = 15700 M^{-1} cm^{-1} in acetonitrile.

[Ru(Ph-T)(dmeb)CN]PF$_6$. ^{1}H NMR [300 MHz, $(CD_3)_2SO$]: δ 10.16 (d, 1H), 9.34 (s, 1H), 9.24 (s, 2H), 9.16 (s, 1H), 8.97 (d, 2H), 8.43 (d, 1H), 8.33 (d, 2H), 8.10 (t, 2H), 7.73−7.60 (overlapped, 7H), 7.39 (t, 2H), 4.09 (s, 3H), 3.87 (s, 3H). Anal. Found: C, 50.31; H, 3.02; N, 9.56. Calcd for $C_{36}H_{27}F_6N_6O_4PRu\cdot 0.5H_2O$: C, 50.12; H, 3.27; N, 9.74.

[Ru(dma-T)(dmeb)CN]PF$_6$. ^{1}H NMR [300 MHz, $(CD_3)_2SO$]: δ 10.19 (d, 1H), 9.31 (s, 1H), 9.16 (s, 1H), 8.80 (d, 2H), 8.40 (dd, 1H), 8.11 (s, 2H), 8.03 (dd, 2H), 7.75 (d, 1H), 7.71 (d, 1H), 7.64 (d, 2H), 7.32 (dd, 2H), 4.11 (s, 3H), 3.91 (s, 3H), 3.42 (s, 6H). ESI-MS (675.68 calcd for $C_{32}H_{28}N_7O_4Ru^+$) m/z (%): 675.72 (100) [M], 648.70 (50) [M − HCN]. Anal. Found: C, 45.88; H, 3.92; N, 11.06. Calcd for $C_{32}H_{28}F_6N_7O_4PRu\cdot 1.5H_2O\cdot 0.5C_3H_8O$: C, 45.84; H, 4.02; N, 11.17. Molar extinction coefficient: ε (518 nm) = 17800 M^{-1} cm^{-1} in acetonitrile.

[Ru(pyrr-T)(dmeb)CN]PF$_6$. ^{1}H NMR [300 MHz, $(CD_3)_2SO$]: δ 10.22 (d, 1H), 9.31 (s, 1H), 9.16 (s, 1H), 9.03 (d, 2H), 8.93 (s, 2H), 8.78 (d, 2H), 8.40 (d, 1H), 7.77 (broad, 1H), 7.66 (m, 2H), 7.51 (broad, 1H), 7.32 (t, 2H), 4.13 (s, 3H), 3.94 (s, 3H), aromatic and methyl hydrogens only. Anal. Found: C, 47.93; H, 3.87; N, 11.24. Calcd for $C_{34}H_{30}F_6N_7O_4PRu\cdot 0.25H_2O$: C, 47.98; H, 3.61; N, 11.52.

Crystallography. The crystal was a red needle (∼0.18 mm × ∼0.08 mm × ∼0.08 mm) of $C_{32}H_{28}N_7O_4Ru\cdot PF_6\cdot H_2O$ produced by slow evaporation of a solution containing the complex in a 2:1 acetone/*n*-propanal mixture. The programs used for data collection and workup included DENZO/SCALEPACK, XPREP, which determined the space group, and DENZO-SMN.[32] The structure solution program PATTY in DIRDIF99[33] helped determine the structure. The SHELX-97[34] program in conjunction with a LINUX PC platform yielded the final refined structure. Table 1 reports relevant information about data collection as well as figures of merit for the final refinement.

dx.doi.org/10.1021/ic4016367 | *Inorg. Chem.* 2013, 52, 12553−12560

Table 1. Crystallographic Data

molecular formula	$C_{32}H_{30}F_6N_7O_5PRu$
formula weight	838.67
space group	$C2/c$ (No. 15)
a (Å)	39.7766(15)
b (Å)	8.8488(4)
c (Å)	20.6900(7)
β (deg)	101.63(3)
V	7132.6(5)
Z	8
ρ_{calc} (g cm^{-3})	1.562
μ (mm^{-1})	4.787
transmission coefficient	0.539−0.682
T (K)	120
no. of reflections measured	40310
no. of independent reflections	5691
final R indices $[I > 2\sigma(I)]$	$R = 0.038^a$
	$R_w = 0.101^b$

$^aR = \sum||F_o| - |F_c||/\sum|F_o|$ for $F_o^2 > 2\sigma(F_o^2)$. $^bR_w = [\sum w(|F_o^2| - |F_c^2|)^2/\sum w(|F_o^2|)^2]^{1/2}$.

RESULTS

Structure of [Ru(dma-T)(dmeb)CN]$^+$. Figure 1 provides a representation of the structure of [Ru(dma-T)(dmeb)CN]$^+$ along with selected geometric data. Within the structure, the terpyridine moiety is essentially planar, the average magnitude of out-of-plane displacement being 0.0375 Å. The atoms straying farthest from the mean plane are C123 at 0.089 Å and C114 at −0.086 Å. In addition, the C−N−C plane of the dma substituent twists 11.31° out of the plane. Within the dmeb ligand, the torsion angle between the pyridine rings is only 3.88°.

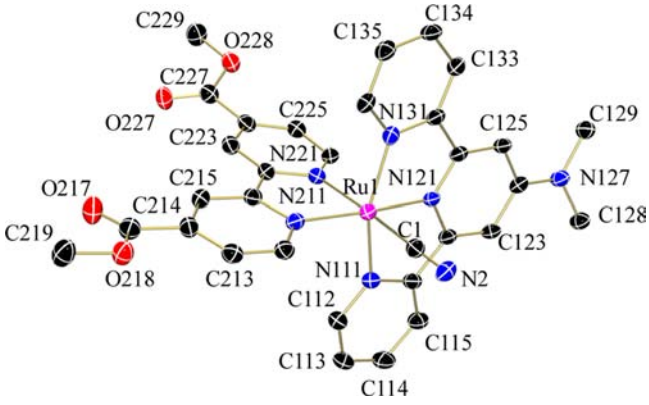

Figure 1. Molecular structure of a representative cation of [Ru(dma-T)(dmeb)CN]$^+$ along with selected geometric data with thermal ellipsoids set at 50% probability. Selected bond lengths (angstroms) and angles (degrees) associated with the metal center: N111−Ru1, 2.073(3); N121−Ru1, 1.978(3); N131−Ru1, 2.081(3); N221−Ru1, 2.090(3); N211−Ru1, 2.066(3); C1−Ru1, 2.009(4); N111−Ru1−N131, 158.04(11); N111−Ru1−N121, 79.40(11); N121−Ru1−N131, 78.65(11); N211−Ru1−N221, 78.62(1); N221−Ru1−C1, 176.03(12).

The -CO_2 plane containing C227 makes a dihedral angle of 21.72° with respect to the attached pyridine, while the other -CO_2 plane makes a dihedral angle of 6.98° with respect to the attached pyridine ring. In line with related [Ru(N^N^N)-(N^N)L]$^{n+}$ systems, the lengths of the bonds to the ligand nitrogens vary.[20,35−37] Most prominently, the Ru−N121 bond to the inner nitrogen of the dma-T ligand is short compared to the others, which are all of fairly similar lengths. One other contrast that may be worth noting is that the bond to N221 of dmeb, which is *trans* to the cyanide ligand, is longer than that of its N211 counterpart. The same trend occurs in the structures of related cyano complexes [Ru(trpy)(bpy)CN]$^+$,[37] [Ru-(dppzp)(bpy)CN]$^+$,[21] and *cis*-Ru(4,4′-^{t}Bu$_2$-bpy)$_2$(CN)$_2$.[38]

Absorbance and Electrochemistry. Table 2 includes a summary of the measured electrochemical potentials and absorbance data. The potential for the first reduction is reasonably constant throughout the [Ru(X-T)(dmeb)CN]$^+$ series and invariably more than 200 mV more positive than the potential for the first reduction of [Ru(trpy)(bpy)CN]$^+$ or [Ru(dma-T)(bpy)CN]$^+$.[21] It is therefore clear that the site of the first reduction is the coordinated dmeb ligand, as has been noted in previous studies of mixed-ligand complexes of ruthenium.[39] The potential for the Ru(III)/Ru(II) couple is at least 2 V more anodic and becomes less positive when the 4′-substituent of the trpy ligand is electron releasing (NMe$_2$ ≈ pyrr). The trend makes sense in terms of an inductive effect and stabilization of the Ru(III) oxidation state.[21,40] Similarly, the CT absorption maximum also varies with the substituent and shifts toward longer wavelengths as the substituent becomes more electron releasing: H < Ph < dma < pyrr.

Photophysics. Table 2 also contains a summary of emission quantum yields and lifetimes measured in acetonitrile. Consistent with the absorbance, the emission maximum shifts to longer wavelengths upon addition of an electron-donating substituent at the 4′-position of the trpy ligand. In contrast to the CT absorption, however, the wavelength of the CT emission maximum and the emission intensity are quite solvent-dependent. For example, Figure 2 reveals that the emission signal from [Ru(Ph-T)(dmeb)CN]$^+$ is stronger when the solvent is DMSO as opposed to DCM, but the reverse is true of [Ru(dma-T)(dmeb)CN]$^+$. In general, the corrected emission signal shifts to longer wavelengths in more polar solvents (Table 3).

Data in Table 3 also reveal that the excited-state lifetime varies dramatically with the solvent. The lifetime correlates with

Table 2. Absorbance and Corrected Emission Maxima Measured in CH_3CN at Room Temperature and Electrochemistry Data from Dimethylformamide

					E_{red} (V)^b		
complex	λ_{abs}^{max} (nm)	λ_{em}^{max} (nm)	$10^3 \times \Phi^a$	τ^a (ns)	2+/+	+/0	0/−
[Ru(trpy)(dmeb)CN]$^+$	497	720	2.6	113	0.71	−1.52	−1.98
[Ru(Ph-T)(dmeb)CN]$^+$	504	731	3.2	110	0.7	−1.59	−1.94
[Ru(dma-T)(dmeb)CN]$^+$	517	789	1.9	60	0.45	−1.56	−2.09
[Ru(pyrr-T)(dmeb)CN]$^+$	520	800	1.5	47	0.45	−1.55	−2.08

^{a}The estimated error in emission yield and lifetime is 10%. ^{b}The reference is Fc$^{+/0}$.

dx.doi.org/10.1021/ic4016367 | Inorg. Chem. 2013, 52, 12553−12560

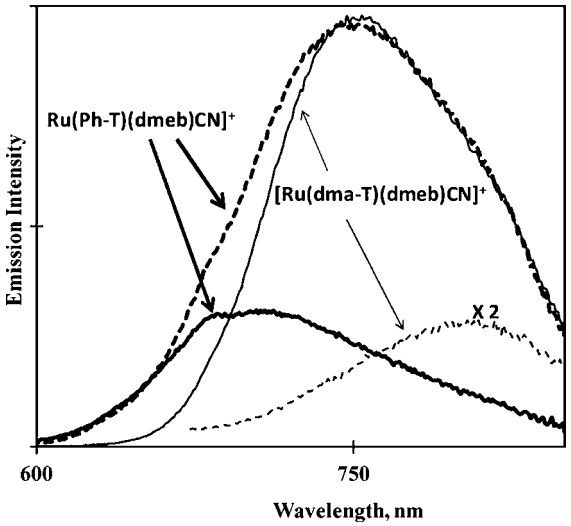

Figure 2. Corrected emission spectra of $[Ru(Ph\text{-}T)(dmeb)CN]^+$ in DCM (thick trace) and DMSO (thick dashed trace) along with $[Ru(dma\text{-}T)(dmeb)CN]^+$ in DCM (thin trace) and DMSO (thin dashed trace, scaled up by a factor of 2). Spectra were recorded at room temperature under a nitrogen atmosphere and normalized to the same absorbance at the excitation wavelength.

Table 3. Corrected Emission Maxima and Lifetime Data for $[Ru(X\text{-}T)(dmeb)CN]^+$ Complexes in Different Solvents at Room Temperature under a Nitrogen Atmosphere

	λ_{em} (nm) [τ (ns)]			
solvent	X = H	Ph	dma	pyrr
DCM	691 (38)	703 (47)	**748 (186)**[a]	**755 (166)**
$CHCl_3$	700 (43)	710 (44)	753 (170)	760 (142)
CH_3CN	720 (113)	731 (110)	789 (60)	800 (47)
DMSO	**746 (163)**	**745 (175)**	800 (34)	800 (34)

[a]Bold data for the solvent that gives the maximal lifetime in each column.

the emission intensity in the sense that the more intense the emission signal, the longer the τ. A survey of Table 3 reveals that each complex achieves an optimum lifetime of 175 ± 10 ns in one solvent or another. More specifically, the excited-state lifetime is optimized when the corrected emission maximum falls near 750 nm.

DISCUSSION

Absorption and Emission Energies. The absorption and emission properties of ruthenium(II) complexes critically depend upon ligand design.[3] For example, $[Ru(trpy)_2]^{2+}$ is a nonemissive complex in a fluid solution, whereas Maestri et al. showed that under the same conditions complexes incorporating appropriately substituted trpy ligands are emissive, albeit weakly.[14] Unsymmetrically substituted systems exhibited the strongest emission signals, the best example being the system with a π-electron-donating -OH group at the 4′-position of one trpy ligand and the electron-accepting $-SO_2CH_3$ group at the 4′-position of the opposing trpy ligand. The authors proposed that the electron-donating group drives up the energy of the dπ highest unoccupied molecular orbital (HOMO) of the complex, while the presence of the opposite electron-accepting group reduces the energy of the ligand-based lowest occupied molecular orbital (LUMO).[14] The net effect is to decrease the energy of the emitting ^{3}CT state vis-à-vis ^{3}d−d states that otherwise quench the emission. Subsequent work on related Ru(II) and Pt(II) systems supports the basic model.[40,41] The impact a substituent has is relatively easy to assess, because the ground-state electrochemistry and the CT absorption and emission processes normally depend upon the same frontier orbitals of ruthenium complexes.[42−44] Thus, in a mixed-ligand complex, the ligand π^* orbital that houses the electron in the lowest-energy CT excited state is the same one populated during ground-state reduction. In the complexes of interest here, that ligand is dmeb, because electrochemistry shows that the presence of the electron-withdrawing ester functions dramatically lowers the energy of its π^* acceptor orbital.[39] In complete accord with this inference, the first reduction potential [E (+/0)] in Table 2 is virtually constant across the entire series. In contrast, the potential for the first oxidation [E (2+/+)] varies significantly depending on the 4′-X group attached to the trpy ligand. Inspection shows that the potential becomes less positive as the electron-releasing ability of the substituent increases: H < Ph < dma ≤ pyrr.[45] For more insight into the HOMO orbital involved, see the Appendix. The upshot is that both the absorption and emission maxima shift to lower energies as the electron donating strength of the 4′-substituent in $[Ru(X\text{-}T)(dmeb)CN]^+$ increases (Table 2).

The other factor that particularly influences the emission energy is the solvent, which responds to solutes on at least two distinct time scales.[24] On a virtually instantaneous time scale, the electron cloud of the solvent is able to polarize and adapt to the changing charge distribution of the solute. This polarization occurs in the ground and excited state, however, and usually does not lead to large changes from solvent to solvent. That probably explains why the CT absorptions of $[Ru(X\text{-}T)(dmeb)CN]^+$ systems are maximized at almost the same wavelength independent of solvent. On a longer time scale, however, the solvent can also change molecular orientation, and the effects can be large depending on the dipole moments involved.[24] To understand the dipole moments in $[Ru(X\text{-}T)(dmeb)CN]^+$ systems, consider Figure 3a. Each complex contains an effective plane of symmetry that bisects the X-T ligand. Accordingly, the ground-state dipole moment resides somewhere in the $y-z$ plane. In the ground state, the dipole moment should be roughly along the z-axis because of the formal positive and negative charges on ruthenium and the cyanide ligand, respectively. In the CT excited state, on the other hand, the magnitude of the dipole moment increases and the negative end rotates toward the y-axis because of the transfer of charge from ruthenium to the dmeb ligand. However, the CT absorption is a Franck−Condon transition, unaffected by solvent reorientation. The emission is different because it occurs on a much longer time scale, and Figure 3b shows that polar solvents differentially stabilize the highly polar CT excited state. The emission therefore shifts to a lower and lower energy as the polarity of the solvent increases.

Lifetime Optimization. At the same time, the nonradiative decay rate, k_n, effectively determines the excited-state lifetime because the emission quantum yield $\Phi \ll 1$. The energy gap law summarizes one important property of the nonradiative rate constant because the emissive CT excited state of a ruthenium polypyridine complex normally has a molecular structure that is very similar to that of the ground electronic state.[23,46−48] If all other factors are the same, the rule is that k_n increases exponentially with a decrease in the energy of the excited state. Equation 1 encodes this effect

dx.doi.org/10.1021/ic4016367 | Inorg. Chem. 2013, 52, 12553−12560

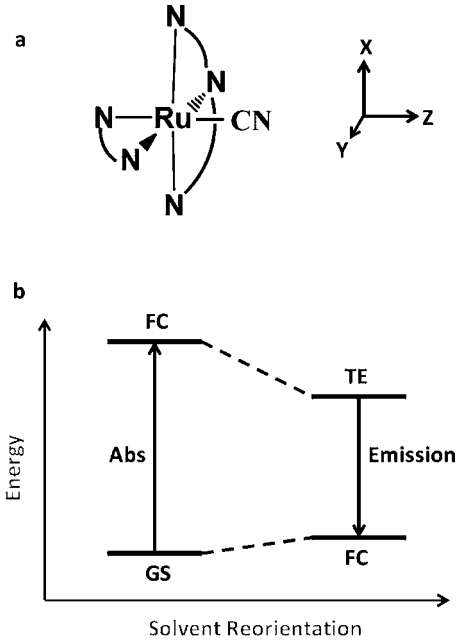

Figure 3. (a) Axis system for the mixed-ligand ruthenium(II) complex. (b) Effect of solvent reorientation and relaxation on state energies. Abbreviations: GS, equilibrated ground state; FC, Franck–Condon state reached with no change in solvent orientation; TE, excited state after thermal equilibration with solvent.

$$k_n = f_n^0 e^{-E/\omega} \quad (1)$$

into equation form, where k_n^0 is a term including a host of factors that collectively determine the maximal relaxation rate, E is the energy of the excited state, and ω is the (average) quantum of energy associated with the ground-state vibrational mode into which the electronic excited state most effectively channels energy.[48,49]

Figure 4 reveals the other important pathway to nonradiative decay in ruthenium(II) polypyridine complexes, namely thermally assisted decay via a higher-energy d–d excited state.[1,3] Indeed, a very efficient k_n' pathway explains why $Ru(trpy)_2^{2+}$, itself, is nonemissive in a fluid solution.[3,5] By introducing a donor group at the 4′-position of one of the trpy ligands and an acceptor group at the 4′-position of the other

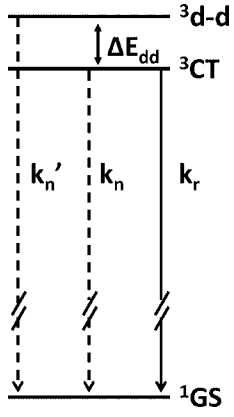

Figure 4. Decay pathways for the emissive ^{3}CT excited state. Radiationless decay occurs directly to the ground state with rate constant k_n or via a thermally accessible d–d state with rate constant k_n'. The rate constant for the radiative pathway is k_r.

trpy, Maestri et al. were able to increase the thermal barrier to quenching ($E_{dd} - E$) and achieve a maximal lifetime of ~50 ns in a room-temperature solution.[14] Heinze et al. used a similar strategy to realize weak emission signals from $Ru(X\text{-}T)(Y\text{-}T)^{2+}$ systems, as well, but provided no lifetime data.[50] The approach taken here with $[Ru(X\text{-}T)(dmeb)CN]^+$ complexes is similar. One simplification is that each system employs the same dmeb acceptor ligand, which turns out to be a rarely used strategy for electronic tuning.[51] Including the strong-field cyanide ligand in the coordination sphere achieves two ends: It minimizes the chance of ligand replacement occurring, and it helps drive up the energies of potentially deactivating d–d states. From the lifetime data obtained, one can estimate the total nonradiative decay rate as $1/\tau \approx k_n + k_n' \approx k_d$, where k_d is the measured rate constant. Again, this approximation recognizes that the radiative pathway (k_r path) makes a negligible contribution to the total decay rate. Within this limit, eq 2 provides a theoretical expression for the rate constant for decay

$$\frac{1}{\tau} = k_n^0 e^{-E/\omega} + A e^{-(E_{dd}-E)/(kT)} \quad (2)$$

where A is a frequency factor for the thermally activated pathway. Making the assumption that E_{dd} is fixed reduces the number of variables and is in accord with the idea that d–d excited states are nonpolar and have energies that are not explicitly dependent on solvent. One can show that when E_{dd} and temperature are constant, the E_{dd} term will actually factor into the pre-exponential parameter A of eq 2. However, it is instructive to retain the form of eq 2 and input a fixed value for E_{dd}. A suitable choice is 2.025 eV, the measured value for $[Ru(trpy)(dmeb)CN]^+$ in a nitrile medium (Figure S1 of the Supporting Information). Even with only three variable parameters, however, there is no unique fit of the experimental data, because of correlation among the variables. A typical fit appears in Figure 5, and it assumes a literature-inspired value for ω of 0.161 eV, or 1300 cm^{-1}.[3,48] This choice is plausible because the cited work suggests that acceptor modes around that frequency are mainly responsible for mediation of nonradiative decay in ruthenium polypyridines. They correspond to framework vibrations of the ligand, but it is worth

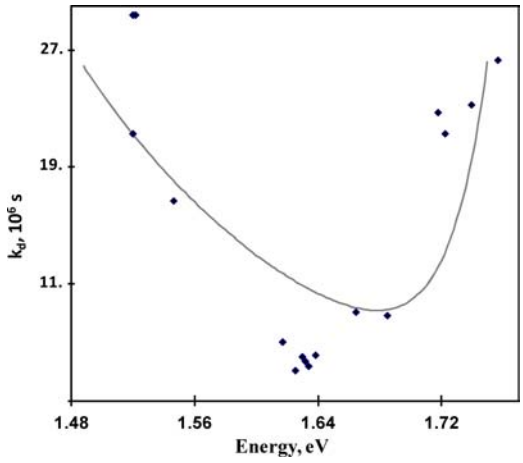

Figure 5. Plot of k_d values vs emission energy: experimental points (◆) and the optimized fit to eq 2 (—). Input values into eq 2 are as follows: E_{dd} = 2.025 eV, and ω = 0.161 eV. Parameter estimates obtained from the fit are as follows: $k_n^0 = 2.64 \times 10^{11}$ s^{-1}, and $A = 1.14 \times 10^{12}$ s^{-1}.

dx.doi.org/10.1021/ic4016367 | Inorg. Chem. 2013, 52, 12553–12560

noting that solvent modes can also influence decay.[23,52] In the case of a dmeb complex, vibrational modes involving the electronically active carboxyester substituents may be important, as well. For comparison, Figure S3 of the Supporting Information presents another fit, which assumes ω = 800 cm^{-1} and produces virtually the same χ^2 value. One deficiency of the model could be that k_n^0 is not actually constant across the series. The complexes would only have the same k_n^0 value if the orbital parentage of the excited state and the spin−orbit coupling interaction remained constant, whereas an admixture of intraligand CT excitation becomes possible when a strong donor substituent is present.[53] The model also assumes that the other pre-exponential A is constant, which means that none of the emitting CT states can begin to equilibrate with the deactivating d−d state.[54,55] Finally, this treatment ignores the possibility that other CT states may be thermally accessible.[6,56] In spite of all the possible shortcomings, the data in Figure 5 reveal that the simple model successfully rationalizes key trends in the nonradiative decay pathway.

OVERVIEW

Heteroleptic complexes of ruthenium(II) involving a combination of monodentate, bidentate, and tridentate ligands have proven to be useful for a variety of applications, including ones that rely on luminescence. This study of [Ru(X-T)(dmeb)CN]$^+$ systems reveals that varying the π-electron-donating ability of the 4′-X substituent of the trpy ligand is an effective way to tune the energy and lifetime of the ^{3}CT emission. Figure 6 illustrates that the maximal room-temperature lifetime that

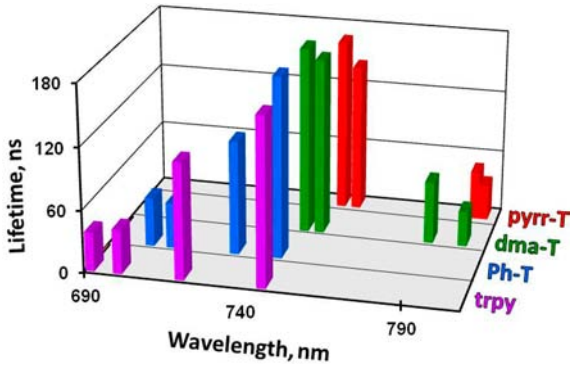

Figure 6. Bar graph of lifetime data for [Ru(X-T)(dmeb)CN]$^+$ complexes. The lifetime increases up the vertical axis, and from front to back, the tridentate ligand ranges from trpy to Ph-T to dma-T to pyrr-T. There are four entries for each row because the lifetime and emission maximum vary with the solvent; the polarity always increases, from left to right from DCM to $CHCl_3$ to MeCN to DMSO, while the emission wavelength is also increasing.

can be obtained in a fluid solution is ∼175 ns, quite an improvement over the prototype [Ru(trpy)(bpy)CN]$^+$ system.[19,21] With the dmeb ligand in place to accept the electron, improving the donor ability of the 4′-X substituent lowers the energy of the ^{3}CT state and reduces the possibility of thermally activated decay via a higher-energy d−d state. Of course, at sufficiently long wavelengths, direct nonradiative decay to the ground state begins to limit the lifetime. Note that in polar solvents, where the emission occurs at relatively long wavelengths, the excited-state lifetimes actually exhibit energy-gap-law behavior (Table 3). However, it is equally obvious that the opposite trend occurs in nonpolar solvents when the emitting states begin to encroach on deactivating d−d states. For these systems, the upshot of the two opposing energy-dependent deactivation pathways is an optimal emission wavelength of ∼750 nm. Perturbations that shift the emission to either a longer or a shorter wavelength inevitably have a negative impact on the excited-state lifetime. Achieving even longer lifetimes will require a modified design, perhaps beginning with a tridentate ligand that supports an expanded bite angle and higher-energy ^{3}d−d states.[12]

Incorporating a trpy analogue that involves carbene donor centers could also be effective.[10] Still another option would be to incorporate a substituent that introduces a lower-energy, ligand-based excited state that has a longer excited-state lifetime if only because of reduced metal participation.[3,45,57−59] In the latter case, the observed lifetime is, however, no longer intrinsic to the CT excited state. Systems with polar emitting states, like [Ru(X-T)(dmeb)CN]$^+$, are extremely versatile because it is possible to tune the emission energy by varying the substituent X or simply changing the solvent.

APPENDIX

The literature reveals that the presence of a 4′-substituent can markedly influence the nature of the HOMO. Consider first the unsubstituted system [Ru(trpy)(bpy)CN]$^+$. Published calculations suggest that the HOMO of the complex involves the d(xz) orbital of ruthenium, when expressed in terms of the axis system presented in Figure 3a.[37] In essence, the HOMO is a mixture of the d(xz) orbital, a π orbital of the cyanide coligand, and a χ-type molecular orbital of the trpy ligand. [Orgel proposed the convention that a π-molecular orbital of a polypyridine ligand be labeled χ (ψ) if it is antisymmetric (symmetric) under reflection through the plane that bisects the ligand.[60]] A χ orbital interacts with the metal via the pπ atomic orbitals of the N and N″ atoms of the trpy moiety, whereas a ψ-type molecular orbital interacts via the pπ atomic orbital of N′. The d(xz) orbital also helps shape the HOMO's of [Ru(trpy)(bpy)Cl]$^+$ and [Ru(trpy)$_2$]$^{2+}$.[61,62] In contrast, Robson et al. showed that the d(yz) orbital participates in the HOMO when the trpy ligand has an electron-donating p-diphenylaminophenyl substituent at the 4′-position.[53] The pπ orbital of the substituent nitrogen also participates in the HOMO as part of a ψ-type orbital of trpy. The accompanying shift in the relative energies of the dπ orbitals may imply that the energy of the d−d excited state also changes when an electron-donating group is present, i.e., in systems containing dma-T or pyrr-T. However, simulations reveal the fit to eq 2 is quite insensitive to the energy of the d−d state for those systems, because the emission decreases at lower energies where energy-gap-law considerations dominate.

ASSOCIATED CONTENT

Supporting Information

X-ray data for [Ru(dma-T)(dmeb)CN]PF_6·H_2O in CIF format, additional emission data, including emission maxima in energy units, information about the E_{dd} value for [Ru(trpy)(dmeb)CN]$^+$, and another fit of the experimental k_d values. This material is available free of charge via the Internet at http://pubs.acs.org.

AUTHOR INFORMATION

Corresponding Author

*E-mail: mcmillin@purdue.edu.

Notes

The authors declare no competing financial interest.

■ ACKNOWLEDGMENTS

The National Science Foundation funded this research via Grant CHE 0847229. We are grateful to Dr. Tong Ren for the use of electrochemical equipment and to Julia Savchenko for technical assistance.

■ REFERENCES

(1) Juris, A.; Balzani, V.; Barigelletti, F.; Campagna, S.; Belser, P.; Vonzelewsky, A. *Coord. Chem. Rev.* **1988**, *84*, 85−277.
(2) Kalyanasundaram, K. *Photochemistry of Polypyridine and Porphyrin Complexes*; Academic Press: New York, 1992.
(3) Campagna, S.; Puntoriero, F.; Nastasi, F.; Bergamini, G.; Balzani, V. *Top. Curr. Chem.* **2007**, *280*, 117−214.
(4) Winkler, J. R.; Netzel, T. L.; Creutz, C.; Sutin, N. *J. Am. Chem. Soc.* **1987**, *109*, 2381−2392.
(5) Hecker, C. R.; Gushurst, A. K. I.; McMillin, D. R. *Inorg. Chem.* **1991**, *30*, 538−541.
(6) Amini, A.; Harriman, A.; Mayeux, A. *Phys. Chem. Chem. Phys.* **2004**, *6*, 1157−1164.
(7) Figgis, B. N.; Kucharski, E. S.; White, A. H. *Aust. J. Chem.* **1983**, *36*, 1563−1571.
(8) Pyo, S.; Perez-Cordero, E.; Bott, S. G.; Echegoyen, L. *Inorg. Chem.* **1999**, *38*, 3337−3343.
(9) McGuire, R.; McGuire, M. C.; McMillin, D. R. *Coord. Chem. Rev.* **2010**, *254*, 2574−2583.
(10) Brown, D. G.; Sanguantrakun, N.; Schulze, B.; Schubert, U. S.; Berlinguette, C. P. *J. Am. Chem. Soc.* **2012**, *134*, 12354−12357.
(11) Medlycott, E. A.; Hanan, G. S. *Coord. Chem. Rev.* **2006**, *250*, 1763−1782.
(12) Abrahamsson, M.; Jager, M.; Osterman, T.; Eriksson, L.; Persson, P.; Becker, H. C.; Johansson, O.; Hammarstrom, L. *J. Am. Chem. Soc.* **2006**, *128*, 12616−12617.
(13) Wadman, S. H.; Tooke, D. M.; Spek, A. L.; van Klink, G. P. M.; van Koten, G. *Inorg. Chim. Acta* **2010**, *363*, 1701−1706.
(14) Maestri, M.; Armaroli, N.; Balzani, V.; Constable, E. C.; Thompson, A. *Inorg. Chem.* **1995**, *34*, 2759−2767.
(15) Hecker, C. R.; Fanwick, P. E.; McMillin, D. R. *Inorg. Chem.* **1991**, *30*, 659−666.
(16) Schofield, E. R.; Collin, J. P.; Gruber, N.; Sauvage, J. P. *Chem. Commun. (Cambridge, U.K.)* **2003**, 188−189.
(17) Goldbach, R. E.; Rodriguez-Garcia, I.; van Lenthe, J. H.; Siegler, M. A.; Bonnet, S. *Chem.—Eur. J.* **2011**, *17*, 9924−9929.
(18) Rachford, A. A.; Rack, J. J. *J. Am. Chem. Soc.* **2006**, *128*, 14318−14324.
(19) Belser, P.; Vonzelewsky, A.; Juris, A.; Barigelletti, F.; Balzani, V. *Gazz. Chim. Ital.* **1985**, *115*, 723−729.
(20) Rasmussen, S. C.; Ronco, S. E.; Mlsna, D. A.; Billadeau, M. A.; Pennington, W. T.; Kolis, J. W.; Petersen, J. D. *Inorg. Chem.* **1995**, *34*, 821−829.
(21) Stewart, D. J.; Fanwick, P. E.; McMillin, D. R. *Inorg. Chem.* **2010**, *49*, 6814−6816.
(22) Parker, C. A.; Rees, W. T. *Analyst (Cambridge, U.K.)* **1960**, *85*, 587−600.
(23) Caspar, J. V.; Meyer, T. J. *J. Am. Chem. Soc.* **1983**, *105*, 5583−5590.
(24) Lakowicz, J. R. *Principles of Fluorescence Spectroscopy*, 2nd ed.; Kluwer Academic/Plenum: New York, 1999.
(25) Anderson, P. A.; Deacon, G. B.; Haarmann, K. H.; Keene, F. R.; Meyer, T. J.; Reitsma, D. A.; Skelton, B. W.; Strouse, G. F.; Thomas, N. C.; Treadway, J. A.; White, A. H. *Inorg. Chem.* **1995**, *34*, 6145−6157.
(26) Oki, A. R.; Morgan, R. J. *Synth. Commun.* **1995**, *25*, 4093−4097.
(27) Dellaciana, L.; Dressick, W. J.; Vonzelewsky, A. *J. Heterocycl. Chem.* **1990**, *27*, 163−165.
(28) Gupton, J. T.; Idoux, J. P.; Baker, G.; Colon, C.; Crews, A. D.; Jurss, C. D.; Rampi, R. C. *J. Org. Chem.* **1983**, *48*, 2933−2936.
(29) Cho, Y. H.; Park, J. C. *Tetrahedron Lett.* **1997**, *38*, 8331−8334.
(30) Clark, M. L.; Green, R. L.; Johnson, O. E.; Fanwick, P. E.; McMillin, D. R. *Inorg. Chem.* **2008**, *47*, 9410−9418.
(31) Michalec, J. F.; Bejune, S. A.; Cuttell, D. G.; Summerton, G. C.; Gertenbach, J. A.; Field, J. S.; Haines, R. J.; McMillin, D. R. *Inorg. Chem.* **2001**, *40*, 2193−2200.
(32) Otwinowski, Z.; Minor, W. *Methods Enzymol.* **1997**, *276*, 307−326.
(33) Beurskens, P. T.; Beurskens, G.; deGelder, R.; Garcia-Granda, S.; Gould, R. O.; Smits, J. M. M. *The DIRDIF2008 Program System*; Crystallography Laboratory, University of Nijmegen: Nijmegen, The Netherlands, 2008.
(34) Sheldrick, G. M. *Acta Crystallogr.* **2008**, *A64*, 112−122.
(35) Billadeau, M. A.; Pennington, W. T.; Petersen, J. D. *Acta Crystallogr.* **1990**, *C46*, 1105−1107.
(36) Gulyas, P. T.; Hambley, T. W.; Lay, P. A. *Aust. J. Chem.* **1996**, *49*, 527−532.
(37) Tsai, C. N.; Allard, M. M.; Lord, R. L.; Luo, D. W.; Chen, Y. J.; Schlegel, H. B.; Endicott, J. F. *Inorg. Chem.* **2011**, *50*, 11965−11977.
(38) Abe, T.; Suzuki, T.; Shinozaki, K. *Inorg. Chem.* **2010**, *49*, 1794−1800.
(39) Barbante, G. J.; Hogan, C. F.; Wilson, D. J. D.; Lewcenko, N. A.; Pfeffer, F. M.; Barnett, N. W.; Francis, P. S. *Analyst (Cambridge, U.K.)* **2011**, *136*, 1329−1338.
(40) Curtright, A. E.; McCusker, J. K. *J. Phys. Chem. A* **1999**, *103*, 7032−7041.
(41) Wilson, M. H.; Ledwaba, L. P.; Field, J. S.; McMillin, D. R. *Dalton Trans.* **2005**, 2754−2759.
(42) Barigelletti, F.; Juris, A.; Balzani, V.; Belser, P.; Vonzelewsky, A. *Inorg. Chem.* **1987**, *26*, 4115−4119.
(43) Curtis, J. C.; Meyer, T. J. *Inorg. Chem.* **1982**, *21*, 1562−1571.
(44) Dodsworth, E. S.; Lever, A. B. P. *Chem. Phys. Lett.* **1984**, *112*, 567−570.
(45) Lazzaro, D. P.; Fanwick, P. E.; McMillin, D. R. *Inorg. Chem.* **2012**, *51*, 10474−10476.
(46) Gelbart, W. M.; Rice, S. A.; Freed, K. F. *J. Chem. Phys.* **1970**, *52*, 5718−5732.
(47) Caspar, J. V.; Sullivan, B. P.; Kober, E. M.; Meyer, T. J. *Chem. Phys. Lett.* **1982**, *91*, 91−95.
(48) O'Neill, L.; Perdisatt, L.; O'Connor, C. *J. Phys. Chem. A* **2012**, *116*, 10728−10735.
(49) Wilson, J. S.; Chawdhury, N.; Al-Mandhary, M. R. A.; Younus, M.; Khan, M. S.; Raithby, P. R.; Kohler, A.; Friend, R. H. *J. Am. Chem. Soc.* **2001**, *123*, 9412−9417.
(50) Heinze, K.; Hempel, K.; Beckmann, M. *Eur. J. Inorg. Chem.* **2006**, 2040−2050.
(51) Kalyanasundaram, K.; Nazeeruddin, M. K. *Chem. Phys. Lett.* **1992**, *193*, 292−297.
(52) Chen, P. Y.; Meyer, T. J. *Chem. Rev.* **1998**, *98*, 1439−1477.
(53) Robson, K. C. D.; Koivisto, B. D.; Gordon, T. J.; Baumgartner, T.; Berlinguette, C. P. *Inorg. Chem.* **2010**, *49*, 5335−5337.
(54) Barigelletti, F.; Juris, A.; Balzani, V.; Belser, P.; Vonzelewsky, A. *J. Phys. Chem.* **1987**, *91*, 1095−1098.
(55) Hewitt, J. T.; Vallett, P. J.; Damrauer, N. H. *J. Phys. Chem. A* **2012**, *116*, 11536−11547.
(56) O'Donnell, R. M.; Johansson, P. R.; Abrahamsson, M.; Meyer, G. J. *Inorg. Chem.* **2013**, *52*, 6839−6848.
(57) Ford, W. E.; Rodgers, M. A. J. *J. Phys. Chem.* **1992**, *96*, 2917−2920.
(58) Simon, J. A.; Curry, S. L.; Schmehl, R. H.; Schatz, T. R.; Piotrowiak, P.; Jin, X. Q.; Thummel, R. P. *J. Am. Chem. Soc.* **1997**, *119*, 11012−11022.
(59) Grusenmeyer, T. A.; Chen, J.; Jin, Y.; Nguyen, J.; Rack, J. J.; Schmehl, R. H. *J. Am. Chem. Soc.* **2012**, *134*, 7497−7506.
(60) Orgel, L. E. *J. Chem. Soc.* **1961**, 3683−3686.
(61) Bomben, P. G.; Robson, K. C. D.; Sedach, P. A.; Berlinguette, C. P. *Inorg. Chem.* **2009**, *48*, 9631−9643.

(62) Jakubikova, E.; Chen, W.; Dattelbaum, D. M.; Rein, F. N.; Rocha, R. C.; Martin, R. L.; Batista, E. R. *Inorg. Chem.* **2009**, *48*, 10720−10725.